Strategy for Seeding 3D Streamlines

Xiaohong Ye* Computer Science Department, UCSC
David Kao† NASA Ames Research Center
Alex Pang‡ Computer Science Department, UCSC

ABSTRACT

This paper presents a strategy for seeding streamlines in 3D flow fields. Its main goal is to capture the essential flow patterns and to provide sufficient coverage in the field while reducing clutter. First, critical points of the flow field are extracted to identify regions with important flow patterns that need to be presented. Different seeding templates are then used around the vicinity of the different critical points. Because there is significant variability in the flow pattern even for the same type of critical point, our template can change shape depending on how far the critical point is from transitioning into another type of critical point. To accomplish this, we introduce the $\alpha-\beta$ map of 3D critical points. Next, we use Poisson seeding to populate the empty regions. Finally, we filter the streamlines based on their geometric and spatial properties. Altogether, this multi-step strategy reduces clutter and yet captures the important 3D flow features.

CR Categories: I.3.6 [Computer Graphics]: Methodology and Techniques—Interaction Techniques;

Keywords: streamlines, flow guided, feature based, filtering, critical points, variable templates

1 INTRODUCTION

The most popular flow visualization method in use today is still streamlines or those derived from streamlines. One of the key issues that affects the quality of streamlines is the seeding strategy as this can lead to clutter, or possibly, visualization artifacts. For the case of streamlines over a planar region or even for 2D manifolds in 3D space, there are two general seeding strategies that offer good solutions to this problem. The first approach is image guided (e.g. [4, 19]) which attempts to distribute streamlines evenly in space by terminating streamlines that are too close to each other, and picking seed points that are at least some distance away from existing streamlines. The second approach is flow guided [20] which attempts to guarantee that important flow features such as those near critical points are clearly shown and seeded first.

For the case of generating streamlines in 3D flow fields, the issue of clutter and occlusion is even more crucial specially when looking at complex flow patterns. The image guided approach was recently extended to visualize 3D flows [10] using evenly spaced illuminated streamlines. To address the issue of clutter, a multi-resolution approach was used wherein streamlines were generated using different separation distances. Sparser streamlines with larger separation distance provided a more global view of the flow field, while denser streamlines with smaller separation distance provided more detail in local regions. Other methods have also been proposed or used, such as seeding based on some physical properties of the flow field, e.g. in regions of high vorticity [13], or level set methods relying on proximity to stream boundaries [22]. However, there is still no systematic study of seeding based on flow characteristics surrounding critical points.

This paper extends and improves upon the flow guided approach to visualize 3D flows in two ways: (i) the seeding template can continuously change shape to best match the flow pattern, and (ii) post process filtering based on geometric and spatial properties of streamlines to reduce clutter. Compared to the multi-resolution, image guided approach, the strategy proposed in this paper can qualitatively capture the important flow features with less streamlines – hence less clutter and occlusion overall. This is because we guarantee that each critical point is represented by a small number of streamlines.

Our seeding strategy involves several steps. We first locate the positions and identify the types of critical points, if any. Then a region of influence is determined around each critical point. Based on this an appropriately scaled template designed to show the flow pattern near each critical point is used to seed some key streamlines. The rest of the volume is seeded using Poisson sphere distributions to fill up the empty space.

As a post processing step, the streamlines can be filtered down to preserve only the more interesting ones. Filtering is done by applying different feature or geometry based criteria successively, e.g. keeping longer streamlines, keeping those with higher winding numbers, removing those which are too close to each other, removing those which are too similar to neighboring ones, etc. Some of the ideas here are extensions of those commonly found in flow simplification work, e.g. where simplification usually occurs based on local flow field properties as opposed to comparison along the length of streamlines [15]. To further improve the spatial perception of the streamlines in 3D, we use illuminated streamlines [23] for rendering. Note that our main goal is to show the important flow features in the data set while reducing clutter and occlusion. Interactivity and speed of generating the seed points and streamlines, while important, are not high priority in this particular report.

2 RELATED WORK

There are several techniques for visualizing 3D volumetric flow fields [6, 11]. Two recent methods addressed both the issue of interactivity and seed placement for streamlines to some degree. Mattausch et al. [10] enhanced the previous seeding algorithms by tapering the ends of the streamlines and introducing interactive halos to improve contrast and spatial perception. For creating evenly spaced streamlines, seeding is also controlled by a minimum distance separation similar to [4]. Further, by varying the separation distance, a multi-resolution seeding strategy is produced, where sparse streamlines are obtained by simply increasing the separation distance, and denser streamlines are obtained by decreasing the separation distance. Laramee et al. [5, 7], used multiple regularly gridded seeding planes that were interactively positioned in the flow field and allowed one to explore the vector field in a similar fashion to the earlier work by Bryson and Levit [3].

However, there is still no systematic way of seeding 3D vector fields. The approach proposed by Mattausch et al. [10] is what Ward [21] refers to as structure-driven. This paper presents how the data-driven or flow guided approach can be extended to 3D flows.

*e-mail: xhye@cse.ucsc.edu
†e-mail:David.L.Kao@nas.nasa.gov
‡e-mail:pang@cse.ucsc.edu

Our method differs from the methods above in that we look at the derived data – the critical points – to determine how the streamlines will be seeded. We use a strategy similar to the topological flow visualization methodology [14] in that we analyze the data set first before trying to visualize it. In contrast to the topological approach where the visualizations are in the form of critical points and separating surfaces [9] or saddle connectors [18], we use the critical point analyses only to determine the important parts of the flow field. The visualization itself is still done with streamlines. We view the methods as complementary. The topological methods provide a global perspective of the vector field, while one still needs to examine regional details using streamlines.

One of the key problems with 3D flow visualization is dealing with occlusion and clutter. Occlusion is inevitable when users are allowed to interactively change their views. View dependent flow visualization that tries to address the occlusion issue may be more distracting than beneficial. A more viable approach is to reduce the clutter in the display. Among the visualization methods using streamlines, there are few methods that address this problem via good streamline seeding strategies – either with minimum distance separation or with clustering. The seeding strategy proposed in this paper guarantees that we will not miss any important flow features derived by local analysis of critical points. And when combined with filtering, we also reduce the clutter and improve the visual presentation. In the next two sections, we look at a multi-step strategy to accomplish these goals.

3 FLOW-GUIDED SEEDING

3.1 Critical Points in 3D

In vector fields, critical points are defined as those points with zero velocity magnitude. Different types of critical points give rise to distinguishing flow patterns in each of their vicinity. A critical point can be classified according to the eigenvalues of its Jacobian matrix $J(p)$ at location p. The positive or negative real part of an eigenvalue indicates whether a streamline seeded near a critical point will attract or repel to the associated eigenvector. If the eigenvalue has a non-zero imaginary part, this streamline may create a spiral structure in the neighborhood of the critical point [1, 2]. Based on the eigenvalues, the different types of critical points in 3D vector fields can be classified into the following basic types shown in Figure 1.

There are ten different types of critical points in 3D flow fields. With the exception of (e1) and (e2), the other eight are stable. Sources (a1) and sinks (a2), while not common in incompressible flows, are accounted for in our study. Aside from these basic critical points, we surmise that there are other "critical regions" in 3D flows. For example, vortex cores are "critical curves" with zero velocity components on the plane normal to the core. In this paper, we do not consider these types of degenerate flow cases but simply focus on those critical points that are defined at a point rather than over a curve or surface.

3.2 Mapping of 3D Critical Points

In order to understand how the flow patterns change with different combinations of eigenvalues, we want to find a mapping that will allow us to study the transition from one type of critical point into another. For this, we need to find a continuous and consistent mapping that reflects the space of possible transitions among critical points shown in Figure 2. More importantly, the mapping should tell us how "close" a critical point is from changing into another type of critical point. This border proximity forms the basis for morphing the seeding templates for flow guided seeding described in the subsequent sections.

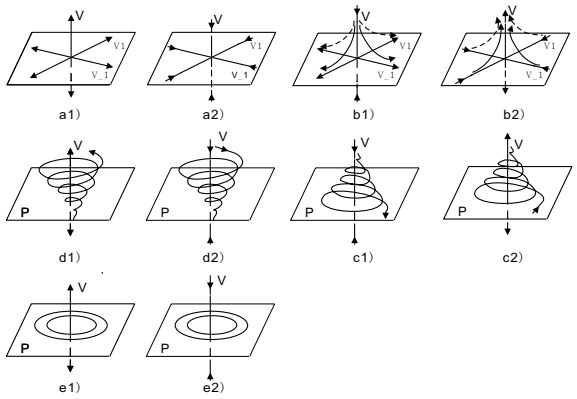

Figure 1: Flows in the vicinity of different types of 3D critical points. (a1) repelling node, (a2) attracting node, (b1) repelling saddle, (b2) attracting saddle, (c1) repelling spiral saddle, (c2) attracting spiral saddle, (d1) repelling spiral, (d2) attracting spiral, (e1) repelling center, and (e2) attracting center.

3.2.1 Mapping

As noted, the three eigenvalues of the Jacobian at a critical point can either be all real numbers, or one is real and the other two are complex conjugate pairs. For the case where the three eigenvalues are all real, we sort them such that $\lambda_1 >= \lambda_2 >= \lambda_3$. For the case where complex numbers are involved, we let the real eigenvalue be c and the complex eigenvalues be $a \pm ib$. We also denote them by the signs of their real parts, e.g. the notation 1-,2+ for a repelling spiral saddle, refers to one negative real, and two complex eigenvalues with positive real parts. Also note that the set of possible transitions of 3D critical points is much more complicated when compared to those of 2D critical points [8, 17].

For 3D critical points, we design the following two-step continuous mapping. In the first step, we map three eigenvalues to three "physical" parameters (x, y, z). When all three eigenvalues are real, we use the following mapping:

$$\begin{aligned} x &= \lambda_1 + \lambda_2 + \lambda_3 \\ y &= min(\lambda_1 - \lambda_2, \lambda_2 - \lambda_3) \\ z &= 2 * \lambda_2 - (\lambda_1 + \lambda_3) \end{aligned} \quad (1)$$

Note that since $\lambda_1 >= \lambda_2 >= \lambda_3$, y is greater or equal to zero. If there exists two equal eigenvalues, then y is equal to zero, and z is equal to $\lambda_2 - \lambda_1$ or $\lambda_2 - \lambda_3$.

In cases that involve complex eigenvalues, we define the following mapping:

$$\begin{aligned} x &= 2a + c \\ y &= b \\ z &= a - c \end{aligned} \quad (2)$$

If b is equal to zero, then all three eigenvalues are real and at least two of them are equal. when two eigenvalues are equal, then y is equal to zero, and z is equal to $\lambda_2 - \lambda_1$ or $\lambda_2 - \lambda_3$. This results in a positive or negative number as z continuously transitions from real to complex eigenvalues. Since the mapping is linear in both real and complex cases, and the transitions are likewise continuous, we have a continuous and homogeneous mapping. Therefore, we

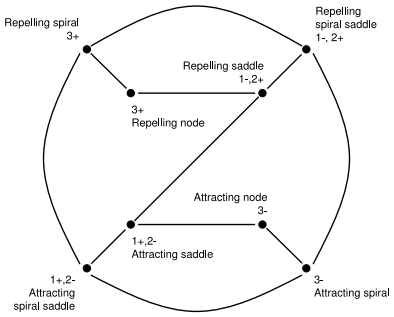

Figure 2: Transition paths from one type of critical point into another. Exterior critical points have eigenvalues with complex conjugates. Interior critical points have eigenvalues that are all real numbers.

can normalize the mapping parameters (x, y, z) to a point on a unit sphere by simply dividing each term by $(x^2+y^2+z^2)^{\frac{1}{2}}$ (see Figure 3). Since we are accounting for the eight stable types of critical points in 3D flow fields, the sphere is subdivided into eight colored regions.

In the second step, we project the unit sphere to a 2D sheet as shown in Figure 4 using (α, β) mapping in Equation 3. With this mapping scheme, every point on this 2D (α, β) space corresponds to a particular critical point.

$$\begin{aligned} \alpha &= \arcsin(y) \\ \beta &= \arctan(\tfrac{z}{x}) + \pi * u(-x) * sign(z) \end{aligned} \tag{3}$$

where $u(-x)$ is 1 when x is less than or equal to zero; otherwise, $u(-x)$ is 0.

This mapping has two sets of degenerate points. Critical points on the bottom edge are degenerate and correspond to the two circular flows in Figure 1. Since these points are unstable in 3D flow fields, we do not consider them further in this paper. Critical points on the top edge are degenerate and reduce to 2D saddles.

The edges separating one region of critical point from another also represent possible transitions between different types of critical points. For example, transitions between repelling saddles and repelling spiral saddles are possible because they share a common edge. Conversely, if two critical points do not share a common edge on these maps, then they cannot transition between these two types directly. For example, repelling saddles cannot change into repelling spirals directly. It needs to change into a repelling node first, then transition into a repelling spiral. The areas corresponding to each type of critical points approximately describe how often they will take place in flow fields.

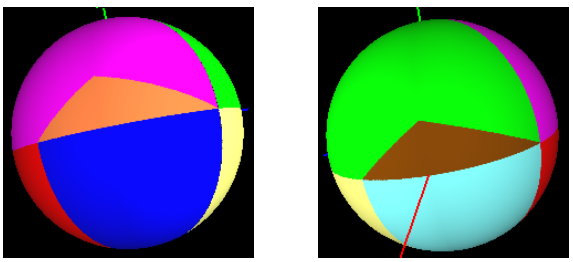

Figure 3: Two viewpoints of the spherical mapping of the three eigenvalues of a critical point to a point on a unit sphere.

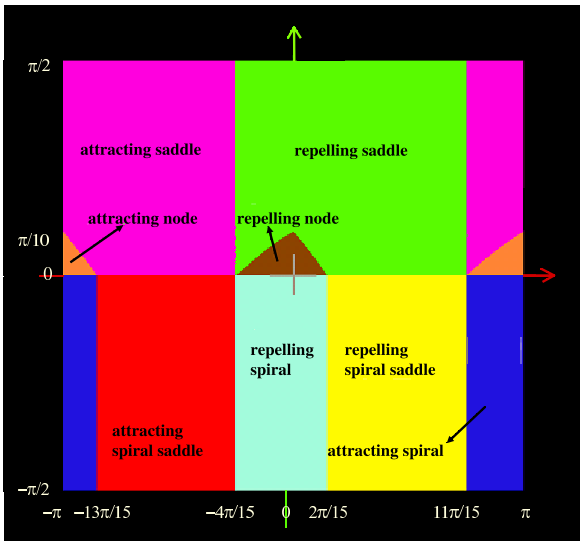

Figure 4: The projection of the unit sphere to a 2D sheet using Equation 3. The ordinate shows values of α, while the abscissa shows values of β.

3.2.2 Inverse Mapping

Given the (α,β) coordinates of a critical point, how can we find the corresponding set of eigenvalues? First, we compute the 3D coordinates of the sphere as following:

$$\begin{aligned} x &= \cos(\alpha) * \cos(\beta) \\ y &= \sin(\alpha) \\ z &= \cos(\alpha) * \sin(\beta) \end{aligned} \tag{4}$$

Where α goes from $\frac{-\pi}{2}$ to $\frac{\pi}{2}$, and β goes from $-\pi$ to π. If y is less than zero, then it is a critical point with complex eigenvalues, and $\| y \|$ is the magnitude of the imaginary part of the complex eigenvalues. From Equation 2, the equations to solve the eigenvalues are:

$$\begin{aligned} a &= \tfrac{x+z}{3} \\ b &= \| y \| \\ c &= \tfrac{x-2*z}{3} \end{aligned} \tag{5}$$

For the case when a critical point has all real eigenvalues, we use Equation 1 to get the the following relationships. If z is less than or equal to zero, the inverse mapping is:

$$\begin{aligned} \lambda_1 &= \tfrac{x-2*z}{3} + y \\ \lambda_2 &= \tfrac{x+z}{3} \\ \lambda_3 &= \tfrac{x+z}{3} - y \end{aligned} \tag{6}$$

When z is greater than zero, we get the following inverse mapping:

$$\begin{aligned} \lambda_1 &= \tfrac{x+z}{3} + y \\ \lambda_2 &= \tfrac{x+z}{3} \\ \lambda_3 &= \tfrac{x-2*z}{3} - y \end{aligned} \tag{7}$$

3.3 Seeding Templates

Since the flow pattern in the vicinity of a critical point is largely defined by the type of critical point, we propose different seeding patterns for different types of critical points. We refer to these seeding patterns as templates. They are designed so that streamlines traced from them can effectively capture the local flow patterns around the critical points. Figure 5 illustrates the seeding templates for the four types of flow patterns: node, saddle, spiral saddle, and spiral.

Recall that the type of the critical point depends on the eigenvalues of the Jacobian matrix J at the critical point. While the sign and magnitude of the eigenvalues determine the divergence or convergence rate of the flow, the related eigenvectors tell us the directions of the streamlines. We use both the eigenvalues and eigenvectors as guides in developing the seeding templates.

1. *Nodes*: We distribute seed points around a circle on two parallel planes on each side of plane P as illustrated in Figure 5 (a). Since the node type critical point is the source or sink of streamlines, the streamlines tend to get cluttered around the critical point. In contrast, the streamlines for saddles don't have this problem near the critical point. They do cluster together along the eigenvectors further away from the critical point.

2. *Saddles*: For the case of saddles, we do not need to place any seeds on plane P. The saddle pattern is brought out by seeding on two parallel planes on opposite sides of plane P. The seeding pattern on these two planes lie on concentric circles whose centers are along V. The number of circles depends on the seeding distance and influence region of the critical point. On each circle, we place eight evenly distributed seed points by default. If the influence region of the critical point is very small, we can reduce the seed points correspondingly. Figure5 (b) shows the seeding template for this type of critical point.

3. *Spiral Saddles*: The spiral flow pattern can be captured by a seeding template where seeds are placed along a line on plane P. The line can be any line other than the eigenvectors spanning P, and is similar to a rake where multiple seeds are placed along its length. This rake is replicated on other planes parallel to P by going some negative and positive distance along V. Figure 5 (c) shows the seed template for spiral saddles. The spacing of the seed points on the rake, the number of planes and spacing of the planes will be discussed in more detail later.

4. *Spiral*: For the typical flow of spiral with large rotations, the streamlines will either wind outward or inward to the critical point. Similar to source and sink nodes, streamlines will congregate near the critical point. Therefore, we use a similar seeding template for spiral saddle as in Figure 5 (d), but with only one seed point on each rake.

The seeding templates described above work for the case where the entire flow field has only one critical point. However, a flow field may also have more than one or no critical points at all. For the case of multiple critical points, the flow pattern associated with a critical point is well defined in its vicinity and weakens as one goes farther away. We discuss how to estimate the influence region for critical points and how to choose the size of the template section 3.5. For the case where there are no critical points, Poisson sphere random seeding with minimum distance separation and/or filtering (see Section 4) seem to be sufficient.

3.4 Variable Templates

The previous section described the four basic seeding templates for the typical flow patterns around different types of critical points.

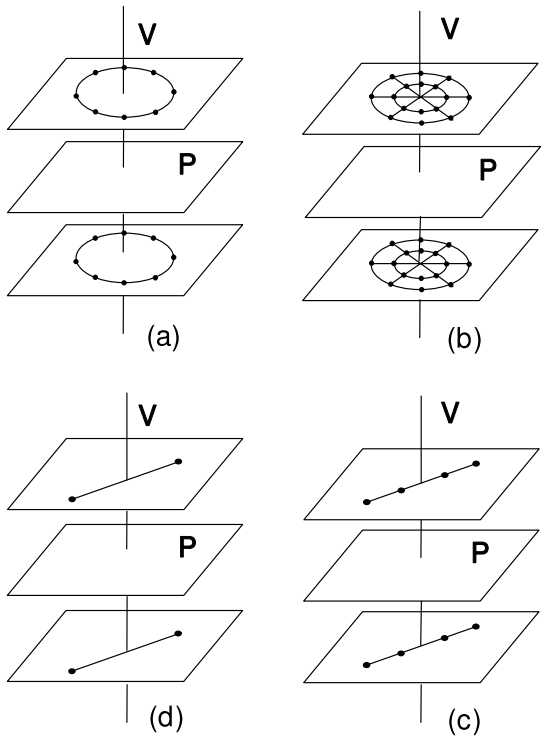

Figure 5: Seeding templates for various critical points. The seeds are placed along the solid lines. The dots represent the seed locations in the templates for: (a) repelling and attracting node (b) repelling and attracting saddle (c) repelling and attracting spiral saddle (d) repelling and attracting spiral The density of the dots can be varied and spaced out differently. The spacing of the planes is also adjusted as a function of the size of the influence region.

Referring to Figure 4, we note that for node and saddle types, the critical points are located on the upper half. Meanwhile, for the spiral and spiral saddle types, the critical points are located on the lower half where $\alpha < 0$. When a critical point is located in the spiral saddle region, but close to saddle region, the flow looks more like a saddle while still possessing winding features. If we use the seeding template for spiral saddle as in Figure 5 (c), we cannot capture the saddle features adequately (see Figure 6 for illustration). In order to overcome this phenomenon, we allow the templates to morph continuously from one type to another.

If we consider the possible transitions of critical points shown in Figure 2 and the corresponding seeding template for each type as shown in Figure 5, then we need to consider four possible morphs amongst the seeding templates. These are:

1. between Figure 5 (a) and (b),

2. between Figure 5 (b) and (c),

3. between Figure 5 (c) and (d), and

4. between Figure 5 (a) and (d),

Due to vertical symmetry along $\beta = -4\pi/15$ in Figure 4, we only consider the repelling types of critical points. This symmetry also allows us to use the same seeding template for an attracting and its corresponding repelling type of critical points.

The number of seed points on a ring for the seeding template of a saddle or node is 8. From $\alpha = 0$ to $\alpha = \pm\frac{\pi}{2}$, we exponentially reduce the number of seeds with the following formula:

$$seedNum = 8 * pow(e, - \parallel \alpha \parallel) \quad (8)$$

This is for the vertical transition between two types of critical points in Figure 4, such as saddle to spiral saddle, and node to spiral. This equation allows us to vary the number of seeds used in the templates between Figure 5 (a) and (d), and between Figure 5 (b) and (c).

For the horizontal transition, such as saddle to node, or spiral saddle to spiral, we linearly increase/decrease the seeding distance of the seed points on each line of the seeding template. This allows us to vary the number of seed used in the templates between Figure 5 (a) and (b), and between Figure 5 (c) and (d). Figures 6 and 7 show the improvement of variable templates in capturing the actual flow patterns of critical points straddling different flow regimes.

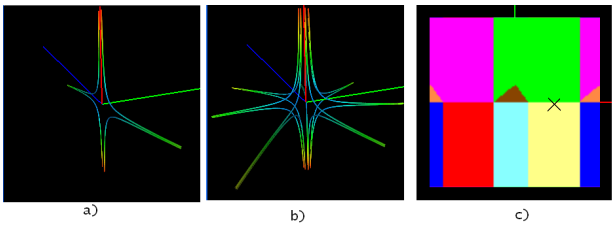

Figure 6: Flow with/without variation in seeding template. The critical point is a repelling spiral saddle, but quite close to a repelling saddle. (a) Seeding with fixed spiral saddle template with 4 seed points. (b) Seeding with variable template with 14 seed points. (c) Location of the critical point marked by X.

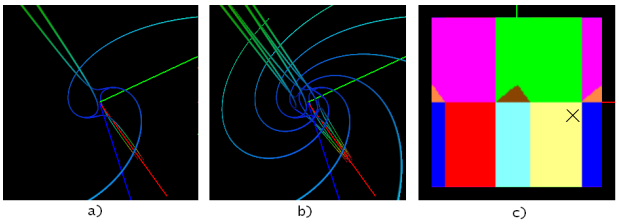

Figure 7: Flow with/without variation in seeding template. The critical point is a repelling spiral saddle, but quite close to an attracting spiral. (a) Seeding with fixed spiral template with 8 seed points (one on each rake). (b) Seeding with variable template with 16 seed points (two on each rake). (c) Location of the critical point marked by X.

3.5 Influence Regions of Critical Points

The main criterion for placing seed points is that we do not miss any important flow features. A conflicting goal is that streamlines do not clutter the display. As such, we want to minimize the amount of seeds yet still show the flow patterns. Since each critical point has a local region of influence where its flow pattern is dominant, we first estimate the region of influence in order to appropriately scale the seeding templates.

For this purpose, the influence region does not have to be accurately computed. Thus, a very simple method would be to take the dimensions of the volume and divide by the number of critical points to get a rough idea of the average size of each influence region. However, in general, critical points are not uniformly distributed in space. Hence, using average sizes will result in overlapping regions. A more accurate method is to do a full topological analyses and calculate the separating regions [9, 18] for each critical point. However, this is quite expensive and is not really necessary for our purpose.

Therefore, for this task, we do not calculate the separating surfaces. Instead, we carry out the following simple procedure for each critical point: (a) find the shortest length from the critical point to the other critical points; let this be L_{min}, (b) set the size of the seeding template for that critical point to $L_{min}/4$. This procedure is quite inexpensive and produces the desired scale factors. Essentially, what we are doing is subdividing the flow domain into sub-domains with one critical point per region. The tessellation is constructed by finding the critical point closest to a given critical point and connecting them with a line. A plane is then constructed at the midpoint and perpendicular to this line. If this is done for every critical point, then the process divides the space into regions. The shortest distance from a critical point to its bounding planes is the "radius" of a region. The size of the seeding template is then set to half of the radius. While this procedure is not fool proof, we have found it quite satisfactory for its intended use.

3.6 Poisson Sphere Seeds

The seeding templates capture the important flow features in the data but do not provide coverage in other areas of the flow. We have to be careful in seeding these other areas because of the potential for clutter. In 3D, clutter is caused by two factors: (a) streamlines getting too close to each other, and (b) viewpoints where streamlines appear to get close to or cross each other. The latter problem cannot be dealt with in a general way other than to reduce their severity either by changing viewpoint or using less streamlines. The former problem can be addressed effectively by enforcing a minimum distance separation between streamlines. This can be done both during the seeding process as well as while the streamline is being traced. For the seeding process, we use a Poisson sphere with radius δ_s for distributing additional seeds beyond those in the seeding templates. These points are placed in the regions outside the influence region of critical points. Note that δ_s is also used as the minimum distance separation for streamline tracing.

4 FEATURE-BASED FILTERING

The main goal of feature based filtering is to reduce clutter. It is carried out by using successive filtering of streamlines based on their geometric and spatial properties. We first define these properties and discuss how they can be applied.

4.1 Geometric Properties of Streamlines

1. *Length:* Before filtering, each streamline is traced completely forward and backward until it is out of the boundary of the flow domain or close enough to a critical point. Associated with each streamline is an accumulated length. The longer a streamline, the more of the flow domain it traverses and the more information or representative it is of the flow. Hence, the length of a streamline is directly proportional to its importance in representing the flow field.

2. *Angle:* In addition to length, every streamline has an accumulated angle, which shows the amount of winding of a streamline. The higher the winding angle, the more interesting the streamline. On the other hand, the winding angle needs to be balanced with the length of the streamline. For example,

a longer streamline may have a larger winding angle than a shorter one, although the shorter streamline may appear to be visually more winding than a longer streamline. The winding angle is calculated as the sum of the angles between two adjacent segments along a streamline.

3. *Proximity to other streamlines:* This is not strictly a property of a streamline per se, but rather gives an indication of the density of streamlines in a local region. An efficient way of storing this information is by maintaining a count of streamlines that pass through a cell or come within a certain distance of a cell. Because flow fields are usually defined on grids, we define a cell count for every cell in the physical space of the flow domain. By looking up the cell count, one can quickly determine the local density of streamlines which also corresponds directly to the degree of clutter in the display.

4.2 Filtering

Filtering can be performed on the basic geometric properties of length and winding angle individually, but can also be based on both criteria at the same time. Different filtering order with the same filtering operations can also produce different results.

In our implementation, streamline filtering is performed in three successive passes. In the first filtering pass, short streamlines with small winding angles are eliminated. These streamlines generally do not contain much information about the flow and tend to produce short discontinuous streamlines that distract the user from the flow pattern.

In the second filtering pass, the output from the first pass is used as the starting point. Here, the streamlines are grouped based on their centroids and endpoints. Those that are similar to each other are removed and only a few representative streamlines are kept. To do this, the streamlines are first sorted by winding angle. If the winding angles of two streamlines are similar, we compare the distance of their endpoints and centroids. If their maximum distance is less than a predefined threshold, one of them is filtered out.

In the third filtering pass, we deal with streamlines with very high winding angles because these streamlines tend to cause visual cluttering in the resultant image. For this pass, we select those cells with both high cell count and streamlines with high winding angles passing through those cells. From this candidate set, we compute the range of the winding angles for these streamlines and group them into different bins. For streamlines in the same bin, we compare the distance between their endpoints, and filter them if the distances are too close to each other. Otherwise, we keep the streamline.

To recapitulate, our multi-step seeding strategy involves the following steps:

1. User specifies a minimum distance separation δ_s.
2. Find the locations and types of critical points.
3. Compute the influence region of the critical points and determine the size of the seeding templates.
4. Scale and morph the seeding templates prior to seeding and tracing streamlines around each critical point.
5. Fill the rest of the space with random seed points that are Poisson sphere distributed.
6. Run successive streamline filtering to reduce clutter.

5 RESULTS AND ANALYSIS

We use both analytical and computational data sets to test our seeding strategy. Analytical data serve to validate as well as stress test our methods since we can vary the number and types of critical points.

Our first analytical test data has five critical points consisting of two spirals, two saddles and one source. This data set is used in two validating tests: (i) compare random seeding against flow guided seeding, (ii) compare dense seeding against filtering.

Figure 8 shows the results of the first test. Note that we kept the number of streamlines the same for fair comparison. Figure 8(a) shows streamlines from randomly placed seeds with Poisson sphere spacing. Figure 8(c) shows streamlines from template seeding followed by Poisson sphere seeding of 22 additional streamlines for an even comparison. Between these two images, the latter image is better because: (i) it shows the saddle structures (lower left and upper right) better, and (ii) the streamlines are spaced out more evenly and there is more uniform coverage over the domain.

Figure 9 shows the results of the second test. We start with a dense seeding of the test data shown in Figure 9(a). We then successively filter the streamlines by removing short streamlines with small winding angles shown in Figure 9(b), then removing similar streamlines shown in Figure 9(c), and finally removing streamlines with very high winding angles shown in Figure 9(d). Obviously, Figure 9(d) is much more revealing than Figure 9(a). We also note that we ended up with 54 streamlines in Figure 9(d), roughly the same number as in Figure 8(c). While the results look comparable, we note that filtering alone does not guarantee that we will not miss any of the critical points.

Using a laptop with a Pentium 1.7Ghz CPU and 1GB of ram, The template seeding in Figure 8 took roughly 0.39 seconds to compute, while the filtering operation in Figure 9 took about 18 seconds. The images with denser lines were rendered with illuminated streamlines, while the sparser images were rendered with tubes.

Our second analytical test data is used to stress test our seeding strategy. This time the data set has 108 critical points consisting of 31 spirals, 28 saddles, and 49 spiral saddles. This data set is used to show results of flow guided seeding followed by filtering. For very complex flows such as this data set, the amount of seed points from seeding templates may be too high. Theoretically, one can vary the number of seed points according to the importance of a critical point over the entire flow domain, or alternatively according to the size of its region of influence. However, there would still be a minimum number of seed points per critical point and if indeed the flow is very complex, it may be impossible to avoid over cluttering the display with this seeding strategy alone. We therefore filter the results of flow guided seeding to reduce the visual clutter. Figure 10 compares the results using Poisson seeding alone and our seeding strategy. This clearly demonstrates the benefit of our seeding strategy as it reduced the overall clutter, and yet one can still discern the flows around individual critical points. The combined computation time for template seeding and filtering of this data set took 15.47 seconds on the same laptop.

Our computational data set is the flow past a cylinder with a hemispherical cap. Most the 45 critical points and interesting flows of this data set are near the cylindrical surface. There are 17 spiral saddles, 20 saddles and 5 spirals, and 3 nodes, in this data set. It took about 6.42 seconds to calculate the bottom image of Figure 11. This figure clearly illustrates the benefit of our seeding strategy. For larger images and animations, as well as additional results using other data sets, please visit www.cse.ucsc.edu/research/avis/seed3d.html

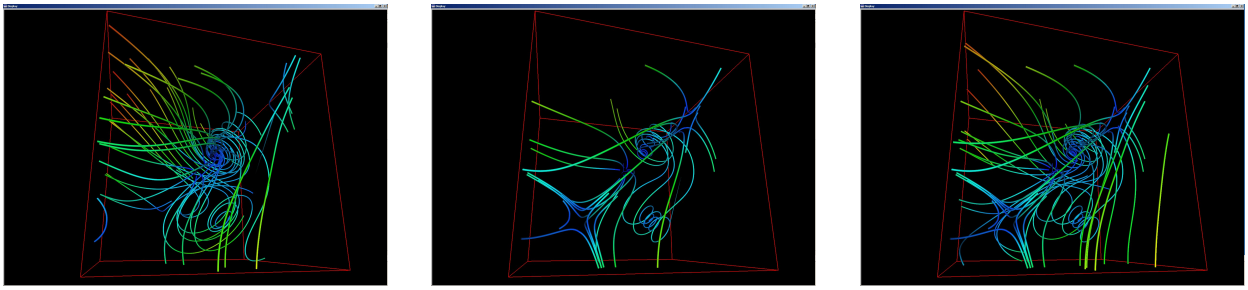

(a) Poisson seeding with 50 streamlines. (b) Template seeding with 28 streamlines. (c) Template then Poisson seeding.

Figure 8: Dataset with five critical points. Colors are mapped to velocity magnitude.

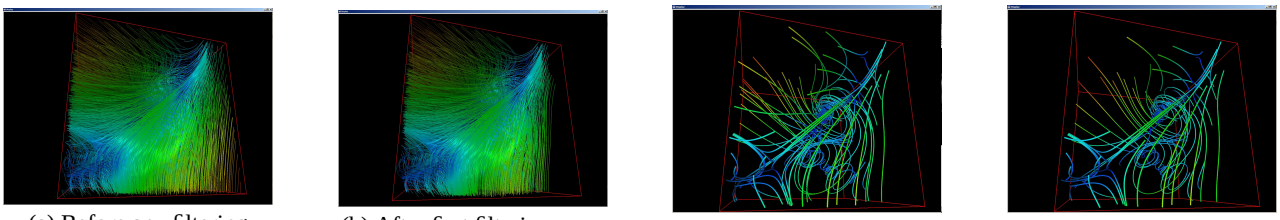

(a) Before any filtering operation; 3168 streamlines. (b) After first filtering pass; 2687 streamlines left. (c) After second filtering pass; 72 streamlines left. (d) After third filtering pass; 54 streamlines left.

Figure 9: Same dataset with five critical points. Colors are mapped to velocity magnitude.

6 DISCUSSION AND FUTURE WORK

In this paper, we presented a multi-step strategy for seeding streamlines in 3D flow fields. Our goal is to highlight the important flow features and reduce clutter. To accomplish this, our strategy involves flow guided seeding followed by successive filtering based on geometric and spatial properties of streamlines. The main strength of flow guided seeding is its ability to capture important flow features in the data set. Its main weakness is its inability to scale up with the complexity (i.e. number of critical points) in the flow data. Filtering does not require prior flow analysis, but can be used either alone or in conjunction with the flow guided seeding strategy. Its main advantage is its ability to deal with large number of streamlines in complex flows, while its main weakness is that there is no guarantee that important flow features are preserved. We combined these two steps in our strategy for seeding 3D streamlines. One of the novel contributions in this work is the mapping of critical points into distinct regions, and using this map to morph our seeding templates to best capture the flow patterns.

There are obviously many directions for improvements. Some of them are: (i) Investigate other forms of data driven seed placement strategies. For example, seeds could be placed in regions of high vorticity, helicity, or pressure gradients, although one may miss other important flow features. In this regard, vector field decomposition, e.g. [12], if extended to 3D, can provide some hints on other types of flow patterns. (ii) Critical point analysis looks at local flow patterns, and may therefore miss global flow patterns such as closed streamlines. Include global flow features in deciding seed placements. (iii) Take advantage of the work on tracking how critical points move and change over time [16], as they provide a relatively smooth way of seeding streamlines in time varying 3D vector fields. (iv) The mapping of three eigenvalues of a critical point is not unique. Investigate other mappings particularly those that are (a) sensitive to the probability of the type of critical point occurring, and (b) where the Euclidean distance from the region boundary is proportional to the "pureness" of the type of critical point for that region. (v) Improve the efficiency of these different automatic flow based seeding methods. The work presented here are just some modest yet useful steps that can be taken right now to reduce the clutter in displays of 3D streamlines.

ACKNOWLEDGMENTS

This project is supported in part by NSF grant ACI-9908881 and NASA Ames through contract # NAS2-03144 for the University Affiliated Research Center under Task Order TO.035.0.DK.INR. Thanks to Xiaoqiang Zheng and Wei Shen for discussions and help with proofreading the paper. Thanks also go to the reviewers for their detailed critiques.

REFERENCES

[1] Daniel Asimov. Notes on the topology of vector fields and flows. Technical Report NASA-RNR-93-003, NASA Ames Research Center, 1993. www.nas.nasa.gov/Research/Reports/Techreports/1993/PDF/rnr-93-003.pdf.

[2] Soumitro Banerjee. Dynamics of physical systems. www.ee.iitkgp.ernet.in/~soumitro/dops, 2004. Online course notes, chapter 6, page 100.

[3] S. Bryson and C. Levit. The virtual windtunnel: An environment for the exploration of three-dimensional unsteady flows. In G.M Nielson and L. Rosenblum, editors, *Proceedings IEEE Visualization '91*, pages 17–24. IEEE Computer Society Press, 1991.

[4] Bruno Jobard and Wilfrid Lefer. Creating evenly-spaced streamlines of arbitrary density. In W. Lefer and M. Grave, editors, *Visualization in Scientific Computing '97*, pages 43–55. Springer, 1997.

[5] Robert S. Laramee. *Interactive 3D Flow Visualization Based on Textures and Geometric Primitives*. PhD thesis, Vienna University of Technology, December 2004.

[6] Robert S. Laramee, Helwig Hauser, Helmut Doleisch, Benjamin Vrolijk, Frits H. Post, and Daniel Weiskopf. The state of the art in

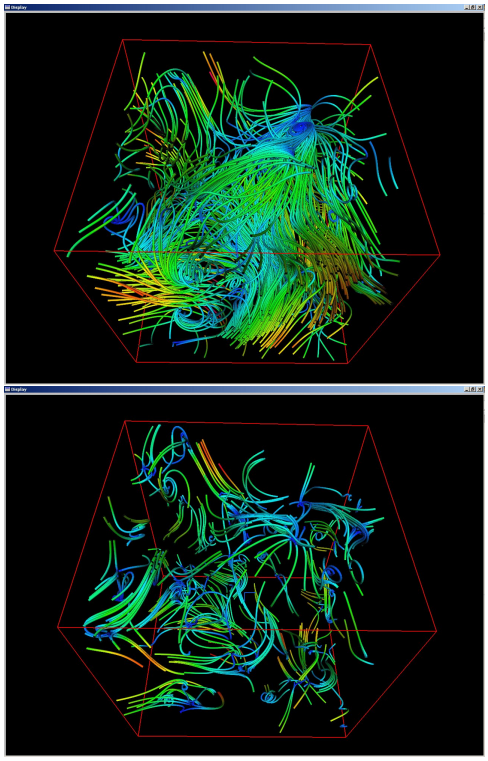

Figure 10: The data set has 108 critical points. The top image shows clutter resulting from Poisson sphere seeding with 403 streamlines. The flow structure is difficult to extract even with interactive viewpoint manipulations. The bottom image used the same data set with template seeding and filtering, with a total of 392 streamlines. The flow structure is now more discernable.

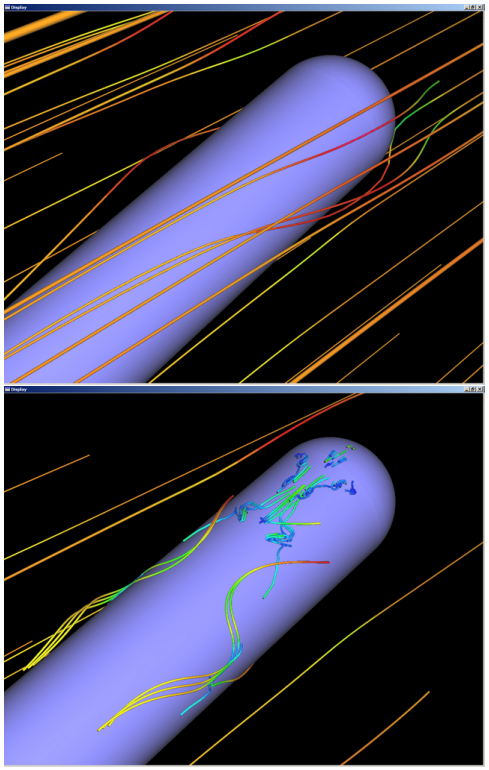

Figure 11: Flow past a cylinder with a hemispherical cap. The top image uses 99 randomly seeded streamlines. The interesting flow patterns near the surface are totally missed. The bottom image uses flow guided seeding followed by filtering, also with a total of 99 streamlines. Attention is now focused on the interesting parts of the flow data.

flow visualization: Dense and texture-based techniques. *Computer Graphics Forum*, 23(2):203–221, 2004.

[7] Robert S. Laramee, Daniel Weiskopf, Juergen Schneider, and Helwig Hauser. Investigating swirl and tumble flow with a comparison of visualization techniques. In *Proceedings of Visualization '04*, pages 51–58, October 2004.

[8] Yingmei Lavin, Rajesh Batra, and Lambertus Hesselink. Feature comparisons of vector fields using earth mover's distance. In *Proceedings of Visualization '98*, pages 103–109, 524, October 1998.

[9] Karim Mahrous, Janine Bennett, Gerik Scheuermann, Bernd Hamann, and Kenneth I. Joy. Topological segmentation in three-dimensional vector fields. *IEEE Transactions of Visualization and Computer Graphics*, pages 198–205, March/April 2004.

[10] Oliver Mattausch, Thomas Theuβl, Helwig Hauser, and Eduard Gröller. Strategies for interactive exploration of 3D flow using evenly-spaced illuminated streamlines. In *Proceedings of Spring Conference on Computer Graphics*, pages 213–222, April 2003. citeseer.nj.nec.com/576694.html.

[11] Frits H. Post, Benjamin Vrolijk, Helwig Hauser, Robert S. Laramee, and Helmut Doleisch. The state of the art in flow visualization: Feature extraction and tracking. *Computer Graphics Forum*, 22(4):775–792, 2003.

[12] Eric Preuβ and Konrad Polthier. Variational approach to vector field decomposition. *Data Visualization (VisSym)*, pages 147–155, May 2000.

[13] Filip Sadlo, Ronald Peikert, and Etienne Parkinson. Vorticity based flow analysis and visualization for pelton turbine design optimization. In *Proceedings of Visualization '04*, pages 179–186, October 2004.

[14] G. Scheuermann and X. Tricoche. Topological methods for flow visualization. In C. Johnson and C. Hansen, editors, *Visualization Handbook*, pages 341–356. Elsevier, 2005. Chapter 17.

[15] A. Telea and J.J. van Wijk. Simplified representation of vector fields. In D. Ebert, M. Gross, and B. Hamann, editors, *Proceedings IEEE Visualization '99*, pages 35–42. IEEE Computer Society Press, 1999.

[16] H. Theisel and H.-P. Seidel. Feature flow fields. In *Proceeding of Joint Eurographics - IEEE TCVG Symposium on Visualization (VisSym '03)*, pages 141–148, 2003.

[17] H. Theisel and T. Weinkauf. Vector field metrics based on distance measures of first order critical points. *Journal of WSCG*, 10:121–128, 2002. wscg.zcu.cz/wscg2002/Papers_2002/D49.pdf.

[18] Holger Theisel, Tino Weinkauf, Hans-Christian Hege, and Hans-Peter Seidel. Saddle connectors - an approach to visualizing the topological skeleton of complex 3D vector fields. In *Proc. IEEE Visualization 2003*, pages 225–232, Seattle, October 2003.

[19] Greg Turk and David Banks. Image-guided streamline placement. In *Proceedings SIGGRAPH*, pages 453–460, New Orleans, LA, August 1996. ACM SIGGRAPH.

[20] Vivek Verma, David Kao, and Alex Pang. Flow-guided streamline seeding strategy. In *Proceedings of Visualization '00*, pages 163–170, 552, 2000.

[21] Matthew O. Ward. A taxonomy of glyph placement strategies for multidimensional data visualization. In *Information Visualization*, volume 1, pages 194–210. Palgrave Macmillan, December 2002.

[22] R. Westermann, C. Johnson, and T. Ertl. A level-set method for flow visualization. In T. Ertl, B. Hamann, and A. Varshney, editors, *Proceedings IEEE Visualization 2000*, pages 147–154. IEEE Computer Society Press, 2000. Flow Visualization.

[23] M. Zöckler, D. Stalling, and H.-C. Hege. Interactive visualization of 3D-vector fields using illuminated streamlines. In *Proceedings of Visualization '96*, pages 107–113, October 1996.